MOLECULAR AND CELLULAR BIOLOGY, Mar. 2011, p. 1145–1159 Vol. 31, No. 6
0270-7306/11/$12.00 doi:10.1128/MCB.00967-10

Derlin-2-Deficient Mice Reveal an Essential Role for Protein Dislocation in Chondrocytes[▽]

Stephanie K. Dougan,[1] Chih-Chi Andrew Hu,[1]† Marie-Eve Paquet,[1]†‡ Matthew B. Greenblatt,[2] Jun Kim,[3] Brendan N. Lilley,[4] Nicki Watson,[1] and Hidde L. Ploegh[1]*

Whitehead Institute for Biomedical Research, 9 Cambridge Center, Cambridge, Massachusetts 02142[1]; Department of Immunology and Infectious Diseases, Harvard School of Public Health, Boston, Massachusetts 02115[2]; Massachusetts Institute of Technology, Cambridge, Massachusetts 02139[3]; and Department of Molecular and Cellular Biology and Center for Brain Science, Harvard University, Cambridge, Massachusetts 02138[4]

Received 18 August 2010/Returned for modification 21 September 2010/Accepted 2 January 2011

Protein quality control is a balance between chaperone-assisted folding and removal of misfolded proteins from the endoplasmic reticulum (ER). Cell-based assays have been used to identify key players of the dislocation machinery, including members of the Derlin family. We generated conditional knockout mice to examine the *in vivo* role of Derlin-2, a component that nucleates cellular dislocation machinery. In most Derlin-2-deficient tissues, we found constitutive upregulation of ER chaperones and IRE-1-mediated induction of the unfolded protein response. The IRE-1/XBP-1 pathway is required for development of highly secretory cells, particularly plasma cells and hepatocytes. However, B lymphocyte development and antibody secretion were normal in the absence of Derlin-2. Likewise, hepatocyte function was unaffected by liver-specific deletion of Derlin-2. Whole-body deletion of Derlin-2 results in perinatal death. The few mice that survived to adulthood all developed skeletal dysplasia, likely caused by defects in collagen matrix protein secretion by costal chondrocytes.

Protein quality control is important: accumulation of misfolded proteins can cause a variety of diseases such as cystic fibrosis, Alzheimer's disease, and spinocerebellar ataxia (8). Protein quality control occurs in all subcellular compartments where misfolded proteins arise or accumulate (cytosol, endoplasmic reticulum [ER], lysosomes, etc.). In the example of cystic fibrosis, cystic fibrosis transmembrane conductance regulator (CFTR), a protein critical for chloride transport, is inactivated by mutations that impair its proper folding. In other cases, accumulation of mutant protein into amyloid aggregates causes disease. Amyloid-induced toxicities are common causes of neurodegenerative diseases such as Parkinson's, Alzheimer's, and Huntington's disease. For each of the known protein quality control diseases, a specific misfolded protein has been identified as the causative agent (8). One might therefore assume that more global defects in protein folding would also lead to pathologies, yet this hypothesis has been difficult to test.

Protein quality control in the ER is achieved through chaperone-assisted folding and by removal of terminally misfolded proteins for destruction via the ubiquitin-proteasome system (24, 31). Folding status is monitored by a large variety of chaperones, and folding itself is regulated by chaperones as well. Misfolded glycoproteins may be recognized by calnexin and calreticulin, which bind to monoglucosylated N-linked glycans. Protein disulfide isomerase (PDI) catalyzes the oxidation and reduction of disulfide bonds and also recognizes nonnative structures. The importance of chaperones in the ER is underscored by the fact that genetic loss of most ER chaperones causes embryonic lethality (31).

If proteins that enter the ER fail to fold properly, they must be removed from the ER, often in a process called dislocation (24). How misfolded proteins are recognized is not completely understood. Proteins with N-linked glycans may be recognized by members of the EDEM (ER degradation-enhancing α-mannosidase-like) protein family which enhance dislocation of certain misfolded proteins (28). The lectin domain-containing OS-9 protein also binds to alternate mannose-containing isomers, as well as to some misfolded proteins that lack N-linked glycans. OS-9 interacts directly with HRD-1 and Sel1L, a ubiquitin ligase complex that interacts with Derlin-1 and Derlin-2 (29, 30). The Derlin family proteins contain four transmembrane domains and are thought to oligomerize in the ER lipid bilayer and may contribute to the formation of a dislocation pore (22, 23, 44). Misfolded proteins are extracted through the action of the cytosolic p97 AAA-ATPase which binds to the Derlins through the adaptor protein VIMP (23, 43). Attachment of at least one ubiquitin moiety is required for recognition by p97 although the ubiquitin is removed prior to full extraction from the ER (23, 43). Several E3 ubiquitin ligases and deubiquitinating (DUB) enzymes have been implicated in dislocation of misfolded proteins; among these are Ubc6e and YOD1 (9, 29).

Cells respond to misfolded proteins via three arms of the unfolded protein response (UPR) (39). PERK, ATF6, and IRE-1 are transmembrane proteins that reside in the ER, functionally coupled to ER quality control machinery. Accu-

* Corresponding author. Mailing address: Whitehead Institute for Biomedical Research, 9 Cambridge Center, Rm. 361, Cambridge, MA 02142. Phone: (617) 324-2031. Fax: (617) 452-3566. E-mail: ploegh@wi.mit.edu.

‡ Present address: Centre de recherche Université Laval Robert-Giffard, 2601 Chemin de la Canardière F6500, Québec, QC, Canada.

† C.-C.A.H. and M.-E.P. contributed equally to this work.

▽ Published ahead of print on 10 January 2011.

mulation of misfolded proteins in the ER can trigger each of these three UPR sensors by as yet poorly defined mechanisms. Activation of PERK results in phosphorylation of eukaryotic translation initiation factor 2α (eIF2α), which causes attenuation of protein synthesis (13). Paradoxically, the ATF4 mRNA, which encodes a transcription factor, is translated better under these circumstances. Increased ATF4 levels lead to transcriptional activation of several ER chaperones, genes involved in amino acid metabolism and transport, and CCAAT/enhancer-binding protein (C/EBP) homologous protein (CHOP) (25). The second UPR sensor, ATF6, is found in the ER and interacts with BiP through its luminal domain. Dissociation from BiP exposes a Golgi localization sequence in ATF6, and once in the Golgi compartment, ATF6 is cleaved by site-1 and site-2 proteases to release the 50-kDa active form of the ATF6 transcription factor, which then translocates to the nucleus (14). ATF6 activates transcription of BiP, XBP-1, various components of ER quality control, and CHOP. IRE-1, evolutionarily the most ancient of the ER stress sensors, is activated upon dimerization and autophosphorylation (4, 36). The cytoplasmic domain of IRE-1 catalyzes an unconventional RNA splicing event to remove a short sequence from XBP-1 mRNA (6). The resulting spliced XBP-1 protein (XBP-1s) translocates to the nucleus and activates transcription of ER chaperones and enzymes involved in lipid biosynthesis to allow expansion of the ER (37).

Knockout mice exist for all three arms of the UPR. *Perk*$^{-/-}$ mice are born at Mendelian ratios but show defects in both the endocrine and exocrine pancreas. They develop overt diabetes by 4 weeks of age (12). Accumulation of misfolded proteins can be observed directly in *Perk*$^{-/-}$ pancreatic islet and acinar cells by electron microscopy, which shows distended, electron-dense ER structures (12). Two *Atf6* genes, *Atf6*α and *Atf6*β are present in mammals, and these have some functional redundancy. *Atf6*α$^{-/-}$ mice are phenotypically normal but develop liver steatosis upon intraperitoneal challenge with tunicamycin (TM) (40). The combined *Atf6*α *Atf6*β double knockout is lethal at a stage prior to embryonic day 8.5, possibly due to an inability to transcribe genes that encode critical ER chaperones such as BiP (42). Indeed, *Bip*$^{-/-}$ mice also die at an early stage of embryonic development (26). Both *Ire-1*α$^{-/-}$ and *Xbp1*$^{-/-}$ mice die around embryonic day 13.5 due to liver failure (33). IRE-1β is expressed primarily in intestinal epithelial cells, and deletion of *Ire1*β renders mice susceptible to sodium dextran sulfate-mediated colitis (3). Conditional ablation of *Xbp1* in B cells or in intestinal epithelial cells uncovered an essential requirement for XBP-1 in formation of plasma cells and Paneth cells, respectively (17, 34). Although XBP-1 induction in B cells occurs independently of unfolded protein accumulation, XBP-1 plays an important role in plasma cell formation through modulation of lipid synthesis, regulation of transcription factor expression, and homing of plasma cells to the bone marrow (16, 27).

Blocking any of the three arms of the unfolded protein response should lead to an increase in misfolded proteins in tissues that are likely to experience ER stress because of a high secretory load. Loss of PERK, ATF6, and IRE-1 pathways primarily affects organs such as the liver and pancreas, as well as specific secretory cell types such as B cells and Paneth cells. Although all arms of the UPR cause upregulation of BiP and other ER chaperones, the majority of transcriptional targets for ATF4, ATF6, and XBP-1s are nonoverlapping (1, 19). Furthermore, different tissues rely on the different UPR components to different extents. As a consequence, *Perk*$^{-/-}$, *Atf6*$^{-/-}$, and *Ire1*$^{-/-}$ mice have quite different phenotypes. In general, however, disruption of any single branch of the UPR has serious adverse consequences.

Here, we report a knockout mouse model of a protein involved in ER dislocation. Derlin-2 interacts with Derlin-1, Sel1L, VIMP, p97, HRD-1, OS-9, and Ubc6e to form a dislocation complex involved in the removal of misfolded substrates from the ER (23, 29, 30). Derlin-2 appears to be more abundant and is present at a higher level than Derlin-1 in the Sel1L-nucleated dislocation complex. Silencing of Derlin-2 impairs dislocation of the null Hong Kong (NHK) version of α1-antitrypsin (32). We show that Derlin-2 deficient mice display constitutive activation of the UPR, and we demonstrate further an unexpected role for Derlin-2 in cartilage formation.

MATERIALS AND METHODS

Animals. Derlin-2 floxed (Derlin-2$^{flox/flox}$) animals were generated by conventional gene targeting (see Fig. 1). Derlin-2 floxed mice were intercrossed with CD19^{cre+}, Alb^{cre+}, or CMV^{cre+} (Cre recombinase driven by the CD19 promoter, the albumin promoter, or the cytomegalovirus [CMV] promoter, respectively) transgenic mice (Jackson Laboratories) to generate *Der2*^{CD19}, *Der2*^{Alb}, and *Der2*$^{-/-}$ mice, respectively. All animals were housed at the Whitehead Institute for Biomedical Research and were maintained according to guidelines approved by the Massachusetts Institute of Technology (MIT) Committee on Animal Care.

Metabolic labeling and pulse-chase experiments. Cells were starved in methionine- and cysteine-free medium containing dialyzed serum for 1 h and then pulse-labeled for 20 min (unless otherwise indicated) with 250 μCi/ml of [^{35}S]methionine and [^{35}S]cysteine (PerkinElmer). At the end of each chase interval, cells were lysed in radioimmunoprecipitation assay buffer containing protease inhibitors. Lysates were then analyzed by immunoprecipitation, SDS-PAGE, and fluorography. Band intensity was determined using a phosphor imager (Fujifilm BAS 2500), and quantitation was done using MultiGauge software (Fujifilm). Hemagglutinin (HA)-agarose beads (Roche) or primary antibodies (Abs) to α1-antitrypsin (Novus Biologicals), major histocompatibility complex class I ([MHC-I] p8), IgM (Southern Biotechnology Associates), or apolipoprotein B (Life span Biosciences) combined with protein G-Sepharose (Sigma) were used for immunoprecipitations.

Antibodies, reagents, and immunoblotting. Cell lysates were prepared using conventional radioimmunoprecipitation assay (RIPA) buffer supplemented with protease inhibitors (Calbiochem). Lysates were clarified at 16,000 × *g* for 10 min at 4°C, resolved by SDS-PAGE (10% acrylamide), and electrophoretically transferred onto a nitrocellulose membrane, which was then blocked with 5% nonfat milk in phosphate-buffered saline (PBS)–0.05% Tween 20, pH 7.4 (PBS-T), before incubation with a primary antibody. After incubation with horseradish peroxidase (HRP)-conjugated secondary antibody (Southern Biotech), the PBS-T-washed membrane was developed using a Western Lightning Chemiluminescence Reagent Plus system (PerkinElmer). The following commercial antibodies were used for immunoblotting: XBP-1 (Santa Cruz), IRE-1α (Cell Signaling), eIF2α (Cell Signaling), actin (Sigma), Derlin-3 (Aviva), calreticulin (Stressgen), p97 (Fitzgerald), OS-9 (Novus Biologicals), HRD-1 (Novus Biologicals), GRP94 (Stressgen), calnexin (Stressgen), α1-antitrypsin (Novus Biologicals), transferrin (Novus Biologicals), MTP (BD), and CHOP (Santa Cruz). Antibodies to Derlin-1, Derlin-2, Sel1L, BiP, Ubc6e, and PDI were generated in our laboratory.

Flow cytometry. The following antibodies for flow cytometry were obtained from BD Pharmingen: IgM (11/41 or R6-60.2), IgD (11-26c.2a), CD1d (1B1), CD19 (MB19-1), CD23 (B3B4), CD43 (1B11), CD138 (281-2), B220 (RA3-6B2), AA4.1, and GL7. Live B cells were stained with the indicated Abs and analyzed by a FACSCalibur flow cytometer (BD Biosciences). Data were analyzed using CellQuest (BD Biosciences).

Cell culture. Mouse embryonic fibroblasts (MEFs) were prepared by dissection and mechanical disruption of embryonic day 14.5 fetuses obtained from pregnant *Der2*$^{+/-}$ females mated to *Der2*$^{+/-}$ males. Livers and hearts

were removed, and the remaining carcass pieces were digested overnight in 0.02% trypsin at 4°C. The tissue pellet was then resuspended in Dulbecco's modified Eagle's medium (DMEM) containing 10% fetal calf serum and plated into 10-cm tissue culture dishes. Individual embryos were genotyped, and all experiments using wild-type and $Der2^{-/-}$ MEFs were performed using MEFs derived from the same litter. Naïve B lymphocytes were purified from mouse spleen by magnetic depletion of CD43-positive cells (Miltenyi Biotech). Naïve B cells were cultured in RPMI 1640 medium containing 10% fetal bovine serum (FBS) with or without lipopolysaccharide (LPS; 20 μg/ml). Primary hepatocytes were isolated and cultured from $Der2^{Alb}$ mice or their Cre-negative littermates. Briefly, mice were anesthetized with an intraperitoneal injection of ketamine (87 mg/kg of body weight; Webster Veterinary, Sterling, MA) plus xylazine (13 mg/kg of body weight; Webster Veterinary). Thereafter, the inferior vena cava was exposed, cannulated, and perfused for 5 min with liver perfusion medium (Invitrogen), followed by a 10-min perfusion with liver digestion medium (Invitrogen), each having been prewarmed to 37°C. The digested liver was diced in cold hepatocyte wash medium (Invitrogen), passed through an 80-μm-pore-size nylon mesh (Sefar-America, Depew, NY), and washed an additional three times. Cells were pelleted and resuspended in cold Williams E medium containing 10% FBS, 10^{-7} M dexamethasone, 10 μg/ml insulin, and 5 μg/ml transferrin. Viability was estimated by trypan blue exclusion, and only preparations with viability in excess of 80% were used for experiments. Cells were plated overnight in six-well Primaria plates (BD Biosciences, San Jose, CA) at a density of 5×10^5 per well. Chondrocytes were isolated from fetal ribs and sternums that had been digested in 2 mg/ml collagenase P (Roche) for 4 h at 37°C. Chondrocytes were centrifuged in 15-ml tubes and cultured as a three-dimensional (3D) pellet in DMEM-F12 medium supplemented with 10% fetal calf serum.

Glucose, triglyceride, and elastase assays. Serum glucose was measured using a One-Touch glucose meter. Serum triglycerides were measured using a triglyceride determination kit (Sigma) as per the manufacturer's instructions. Elastase inhibition was performed using diluted serum as indicated for Fig. 5F and a fixed concentration of porcine elastase in a fluorescence-based activity assay (Invitrogen).

Skeletal preparations. Adult or fetal mice were skinned, eviscerated, and fixed in 95% ethanol. Then skeletons were stained by Alizarin red S/Alcian blue and sequentially cleared in 1% potassium hydroxide.

EM analysis. Chondrocytes in either monolayer or 3D pellet cultures were fixed for electron microscopy (EM) after culturing for 14 days to allow for matrix deposition. The cells were fixed in 2.5% glutaraldehyde and 3% paraformaldehyde with 5% sucrose in 0.1 M sodium cacodylate buffer (pH 7.4). Cells were then postfixed in 1% OsO_4 in veronal-acetate buffer. The cells were stained in block overnight with 0.5% uranyl acetate in veronal-acetate buffer (pH 6.0), dehydrated, and embedded in Spurr's resin. Sections were cut on a Reichert Ultracut E microtome with a Diatome diamond knife at a thickness setting of 50 nm and stained with 2% uranyl acetate, followed by 0.1% lead citrate. Samples were examined using an FEI Tecnai Spirit transmission electron microscope (TEM) at 80 KV and imaged with an Advanced Microscopy Techniques (AMT) camera.

Neuronal imaging. Animals were transcardially perfused with cold phosphate-buffered saline followed by 4% paraformaldehyde in 0.1 M phosphate buffer (PB). Tissue was postfixed with the same fixative and was washed thoroughly with PB. Neural tissue was dissected free and was cryoprotected by sequential overnight incubations in 15% and 30%, wt/vol, sucrose in 0.1 M PB. Tissue was embedded in 22-oxacalcitriol (OCT), frozen, and cut into 20-μm serial sections on a cryostat. Tissue sections were mounted on slides and were stained with cresyl violet or were immunostained with a panel of antibodies. SMI312 antineurofilament monoclonal antibody ([MAb] Covance Research Products) and Alexa Fluor-488 conjugated goat anti-mouse secondary antibodies were used to visualize axon tracts. Epifluorescence and transmitted light images were collected from matched sections from different regions of the brains of two controls and two $Der2^{-/-}$ mice.

Quantitative PCR. Chondrocytes were isolated from embryonic day 18.5 mice. RNA was prepared from freshly isolated chondrocytes or from cells that had been cultured for 14 days. RNA extraction was performed using Trizol (Invitrogen), and cDNA was synthesized using Superscript II (Invitrogen). Quantitative PCR was performed using SYBR green and the following primers: actinF, AGCACAGCTTCTTTGCAGCTCCTT; actinR, CAGCGCAGCGATATCGTCATCCAT; chopF, ACAGAGCCAGAATAACAGCCGGAA; and chopR, TGCTTTCAGGTGTGGTGGTGTATG.

RESULTS

Derlin-2 conditional knockout mice confirm a role for Derlin-2 in ER dislocation. To study the role of Derlin-2 in different tissues, we generated conditional knockout mice in which the Derlin-2 gene is flanked by loxp sites (floxed) (Fig. 1). The resulting Derlin-$2^{flox/flox}$ mouse was crossed to mice expressing Cre recombinase driven by the CMV promoter, by the CD19 promoter, or by the albumin promoter. The resulting $Der2^{-/-}$, $Der2^{CD19}$, and $Der2^{Alb}$ mice have Derlin-2 deleted in all tissues, in B cells, or in hepatocytes, respectively.

Previous work implicating the Derlins in removal of misfolded proteins from the ER has relied on RNA silencing or overexpression of dominant negative Derlin proteins (22, 23, 44). To show by genetic means that Derlin-2 is involved in ER dislocation, we generated mouse embryonic fibroblasts (MEFs) from embryonic day 13.5 Derlin-2-deficient fetuses or their wild-type littermates. $Der2^{-/-}$ MEFs were then transfected with plasmids expressing ribophorin fragment (RI332) or the null Hong Kong (NHK) variant of α1-antitrypsin. RI332 failed to be dislocated at normal rates in $Der2^{-/-}$ MEFs, as shown by ER retention during pulse-chase analysis (Fig. 2A). On the other hand, NHK was dislocated at nearly normal rates, suggesting that Derlin-2 is required for dislocation of a subset of misfolded proteins (Fig. 2B). We found no evidence for a systemic defect in the secretory pathway since properly folded secretory or membrane proteins traverse the ER normally, as shown by equivalent secretion of wild-type α1-antitrypsin and equal maturation of MHC-I (Fig. 2B and C).

$Der2^{-/-}$ MEFs upregulate members of the dislocation complex and have a constitutive UPR. Lysates from two independent wild-type MEF lines (Fig. 3A, first two lanes) and four independent $Der2^{-/-}$ MEF lines (Fig. 3A, last four lanes) were immunoblotted for various ER-resident proteins and proteins involved in the UPR (Fig. 3A). Sel1L, HRD-1, OS-9, and Ubc6e, all members of the Derlin dislocation complex, were upregulated in $Der2^{-/-}$ MEFs. This compensatory upregulation did not apply to Derlin-1; Derlin-1 protein levels were decreased in the absence of Derlin-2 despite increased levels of Derlin-1 transcripts (Fig. 3A and C), suggesting that the loss of Derlin-2 destabilizes Derlin-1 but not other known components of the dislocation complex. Derlin-3 is also expressed in MEFs and B cells but is not affected by loss of Derlin-2. Derlin-3 is more restricted in its tissue expression than the other two Derlins (32); very little Derlin-3 could be detected in liver or chondrocyte lysates (Fig. 3B).

IRE-1α, XBP-1s, BiP, and GRP94 were upregulated in $Der2^{-/-}$ MEFs, indicating induction of the UPR (Fig. 3A). Although the UPR can proceed through three pathways in eukaryotes, the IRE-1 axis seemed to be the only pathway induced in $Der2^{-/-}$ MEFs. ATF6 was not increased (data not shown), and eukaryotic translation initiation factor 2α (eIF2α) phosphorylation was not increased, suggesting that the PERK pathway for UPR induction was not induced by the absence of Derlin-2.

MEF lysates were compared in a side-by-side analysis with lysates from naïve B cells, liver, and chondrocytes (derived from wild-type or $Der2^{CD19}$, $Der2^{Alb}$, or $Der2^{-/-}$ mice, respectively). In all tissues analyzed, Derlin-1 protein levels were decreased in Derlin-2-deficient cells (Fig. 3B). OS-9 and Sel1L

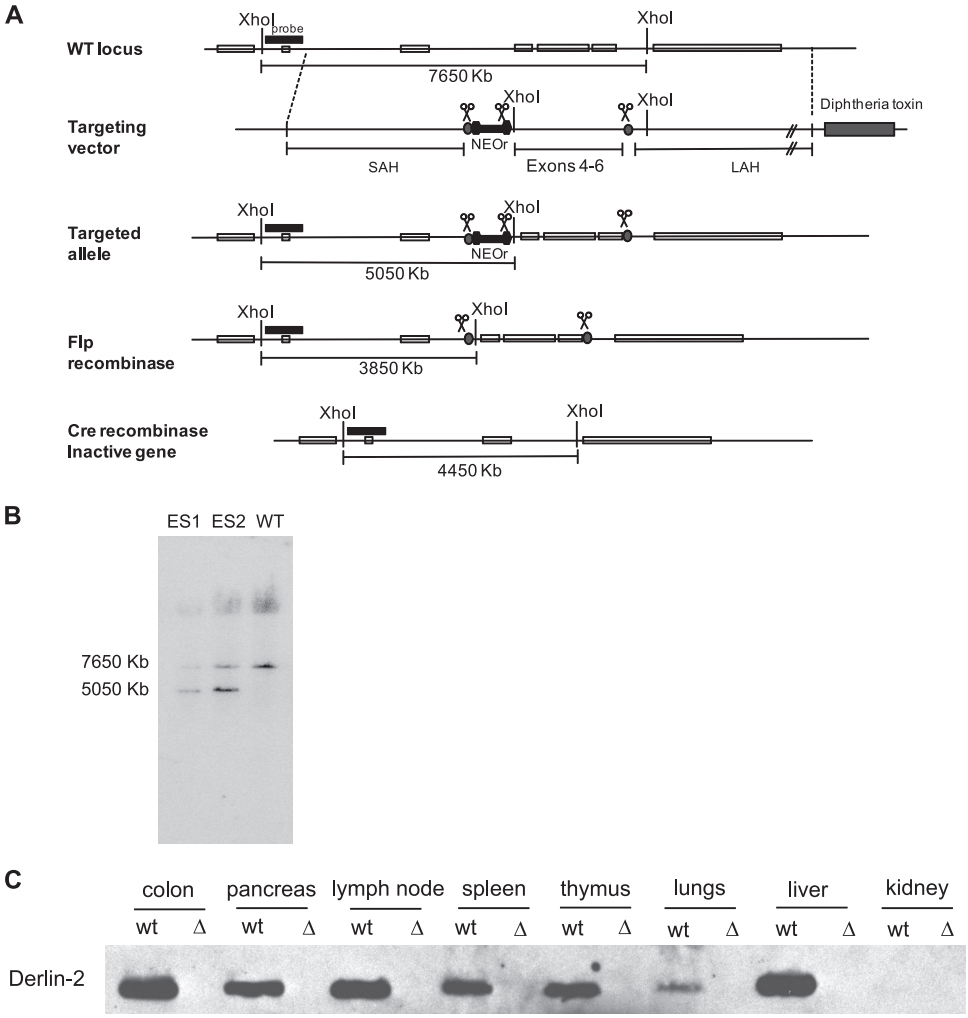

FIG. 1. Generation of Derlin-2 floxed mice. (A) Schematic diagram of the Derlin-2 genomic locus, targeting construct, and genomic locus of the resulting *Der2*$^{-/-}$ mice after Cre-mediated deletion. (B) Genomic DNA was prepared from two lines of targeted embryonic stem cells (ES1 and ES2) or control embryonic stem cells and Southern blotted using the probe indicated in panel A. Correct targeting of the Derlin-2 locus is indicated by the presence of a 5,050-kb band. (C) NP-40 lysates were prepared from the indicated tissues of a *Der2*$^{-/-}$ mouse or littermate control. Samples were subjected to SDS-PAGE and immunoblotted for Derlin-2. WT, wild type.

were upregulated in *Der2*$^{-/-}$ MEFs, liver, and chondrocytes but were affected to a lesser degree in B cells, underscoring the cell and tissue type-specific aspects of the UPR (Fig. 3B).

Loss of Derlin-2 in B lymphocytes has no effect on B cell development or antibody secretion. *Der2*^{CD19} mice were born at normal Mendelian ratios as expected (data not shown). We were particularly interested in the B cell compartment because IRE-1 deficiency affects B cell development (45). B cell subset analysis showed no defects in the percentage or total number of follicular, marginal zone, B-1, transitional T1 or T2, germinal center B cells or plasma cells (Fig. 4A and Table 1) in *Der2*^{CD19} mice: developing B cells in the bone marrow showed normal percentages of pro-, pre-, and immature B cell populations (Table 1).

Upon antigen engagement, naïve B cells develop into antibody-secreting cells and eventually into long-lived plasma cells which continue to secrete antibodies for the remainder of the organism's life. The early stages of this process can be replicated *in vitro* by addition of lipopolysaccharide (LPS), which converts naïve B cells into antibody-secreting B cell blasts. The high rates of immunoglobulin secretion place extreme demands on the functional capacity of the ER. We therefore chose this model as a likely cell type that might reveal even slight perturbations in quality control in the secretory pathway, as has been demonstrated for α1-antitrypsin in fibroblasts. However, metabolic labeling of *Der2*^{CD19} LPS blasts showed no defects in the rates of antibody production or secretion (Fig. 4B and C).

Consistent with the apparent lack of effect of Derlin-2 in B cell development and function, immunoblotting of B cell lysates at various stages of LPS stimulation showed little differences in ER chaperones or dislocation complex members (Fig. 4D), with the exception of Derlin-1, which showed a decrease similar to that seen in MEFs (Fig. 3A and B). Neither IRE-1α nor XBP-1 protein levels were increased in Der2^{CD19} LPS blasts. Loss of Derlin-2 does not obviously enhance UPR ac-

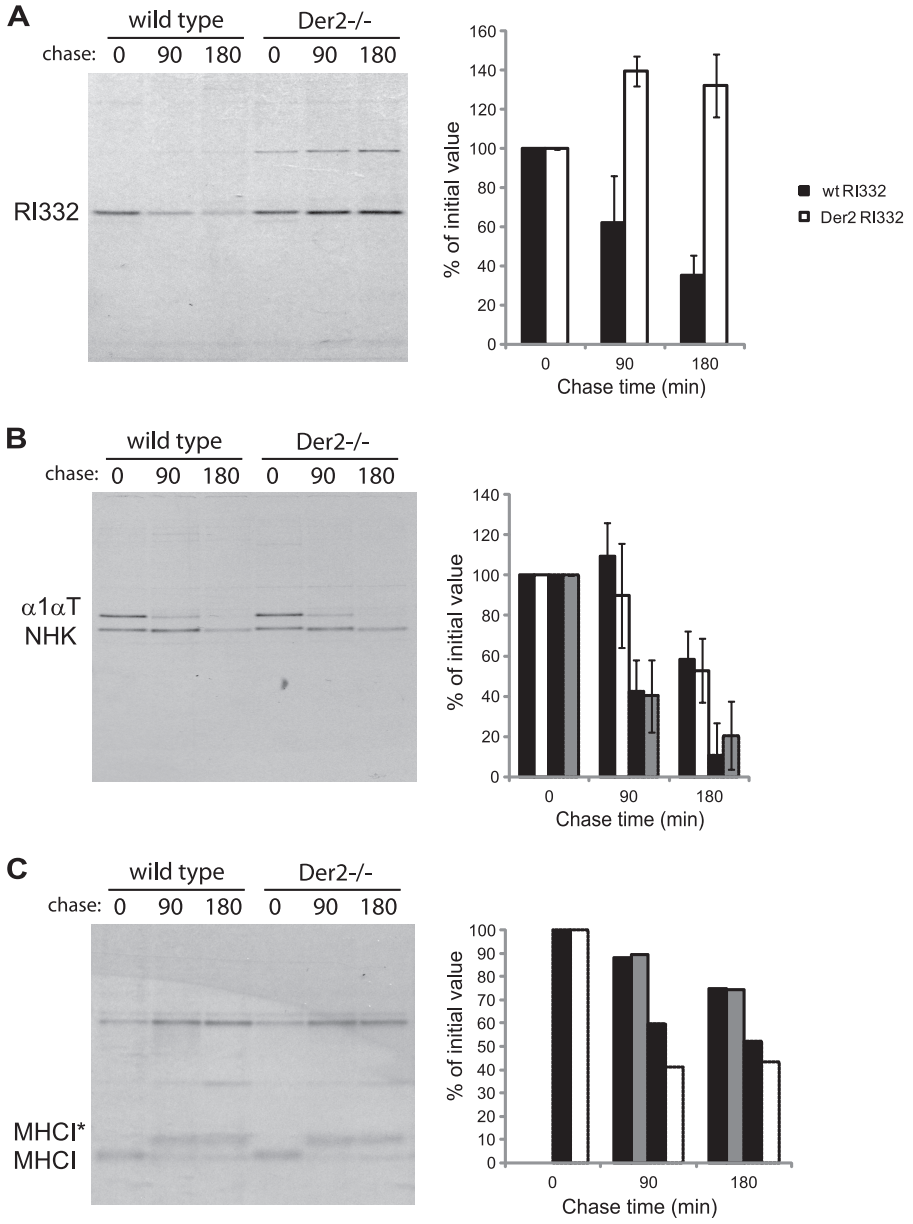

FIG. 2. *Der2*$^{-/-}$ MEFs show impaired protein dislocation. (A) RI332-HA-transfected MEFs were starved for 1 h, pulsed with [^{35}S]cysteine-methionine for 20 min, and chased in nonradioactive medium for the indicated times. Cells were lysed in NP-40 lysis buffer and immunoprecipitated with anti-HA beads. Samples analyzed by SDS-PAGE, and band intensity was quantified using a phosphorimager. A representative gel is shown on the left. Quantification of three independent experiments is shown on the right. (B) MEFs were transfected with HA-α1-antitrypsin (α1αT) and HA-null Hong Kong (NHK) plasmids and subjected to pulse-chase analysis as in panel A. A representative gel is shown on the left. Quantification of three independent experiments is shown on the right. Bars (left to right), wild-type (wt) NHK, *Der2* NHK, wt α1αT, and *Der2* α1αT. (C) MEFs were subjected to pulse-chase analysis as in panel A, and lysates were immunoprecipitated with anti-MHC-I antiserum. Bars (left to right), wt mature MHC-I, *Der2* mature MHC-I, wt immature MHC-I, and *Der2* immature MHC-I.

tivation in developing B cell blasts. By comparison, XBP-1-deficient LPS blasts, which are known to have defects in antibody secretion, show strong upregulation of IRE-1α (Fig. 4D) (16).

Loss of Derlin-2 in hepatocytes has negligible effect on liver function despite an ongoing UPR. *Der2*^{Alb} mice were also born at normal Mendelian ratios (data not shown). No differences were found in serum glucose or serum triglycerides in either fasting (Fig. 5A and B) or fed mice (data not shown). *Atf6α*$^{-/-}$ and *Chop*$^{-/-}$ mice show mild phenotypes at baseline but rapidly succumb to severe liver or kidney disease when challenged with moderate amounts of tunicamycin to induce the unfolded protein response (40, 48). *Der2*^{Alb} mice and their wild-type littermates were injected intraperitoneally with tunicamycin and sacrificed when their body weights reached 80% of baseline. *Der2*^{Alb} mice succumbed at the same rate as control mice (Fig. 5C). Liver lysates from TM-treated mice showed an increase in CHOP and BiP expression, consistent with activation

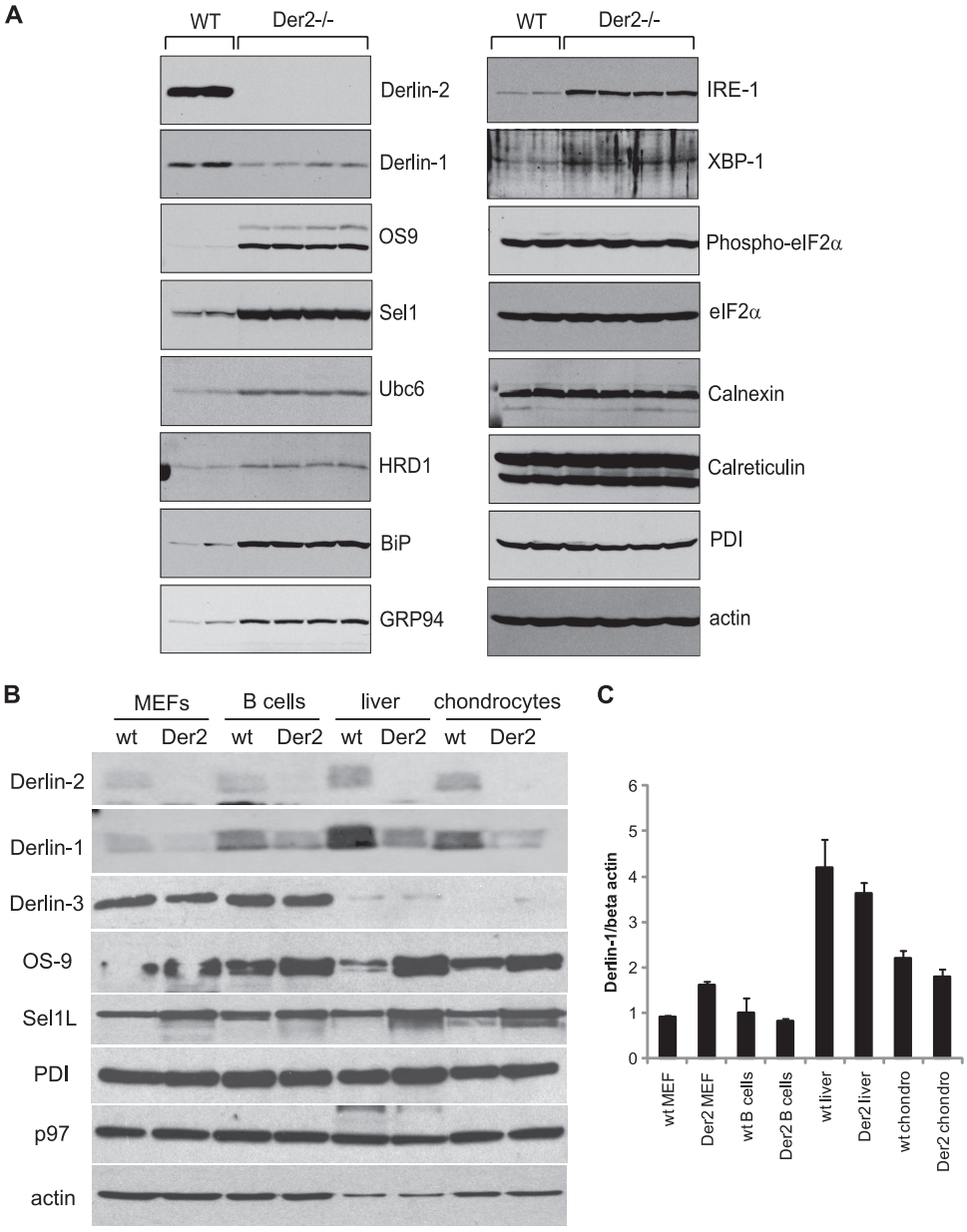

FIG. 3. *Der2*$^{-/-}$ cells upregulate members of the dislocation complex and show a constitutive unfolded protein response. (A) NP-40 lysates from two wild-type (WT) and four *Der2*$^{-/-}$ lines of MEFs were immunoblotted using the indicated antibodies. (B) NP-40 lysates were prepared from MEFs, naïve B cells, freshly isolated hepatocytes, or chondrocytes. Lysates were normalized for total protein content, subjected to SDS PAGE, and immunoblotted using the indicated antibodies. (C) Quantitative PCR was performed using cDNA from the indicated tissues. Derlin-1 transcript levels were normalized to beta-actin. Results are representative of four independent experiments.

of the UPR (Fig. 5D). Sel1L, a glycoprotein that fails to be glycosylated in the presence of TM, was also moderately increased (Fig. 5D). Thus, we conclude that although the TM treatment was effective at blocking glycosylation and inducing the UPR, *Der2*^{Alb} hepatocytes were equally capable as wild type at handling TM challenge. Hepatocytes secrete the majority of serum proteins. We therefore assayed various serum protein levels as a measure of liver secretory function. *Der2*^{Alb} mice showed no signs of anemia (spun hematocrit levels: for *Der2*^{Alb}, 48.2 ± 2.0; for littermate controls, 46.0 ± 2.0) and had normal levels of serum transferrin (Fig. 5E). The levels of α1-antitrypsin were likewise unaffected (Fig. 5E), and a functional assay for inhibition of elastase activity showed no difference (Fig. 5F) between wild-type and *Der2*^{Alb} mice. Total serum albumin was also comparable between *Der2*^{Alb} and control mice (data not shown).

Hepatocyte function is tightly linked to nutrient status; thus hepatocyte lysates were prepared from mice that had been fasted for 24 h and mice that had been fed *ad libitum* (Fig. 5G). Under starvation conditions, normal hepatocytes express less Derlin-2 protein (Fig. 5G). As in MEFs, members of the Derlin dislocation complex Sel1L, HRD-1, and Ubc6e showed

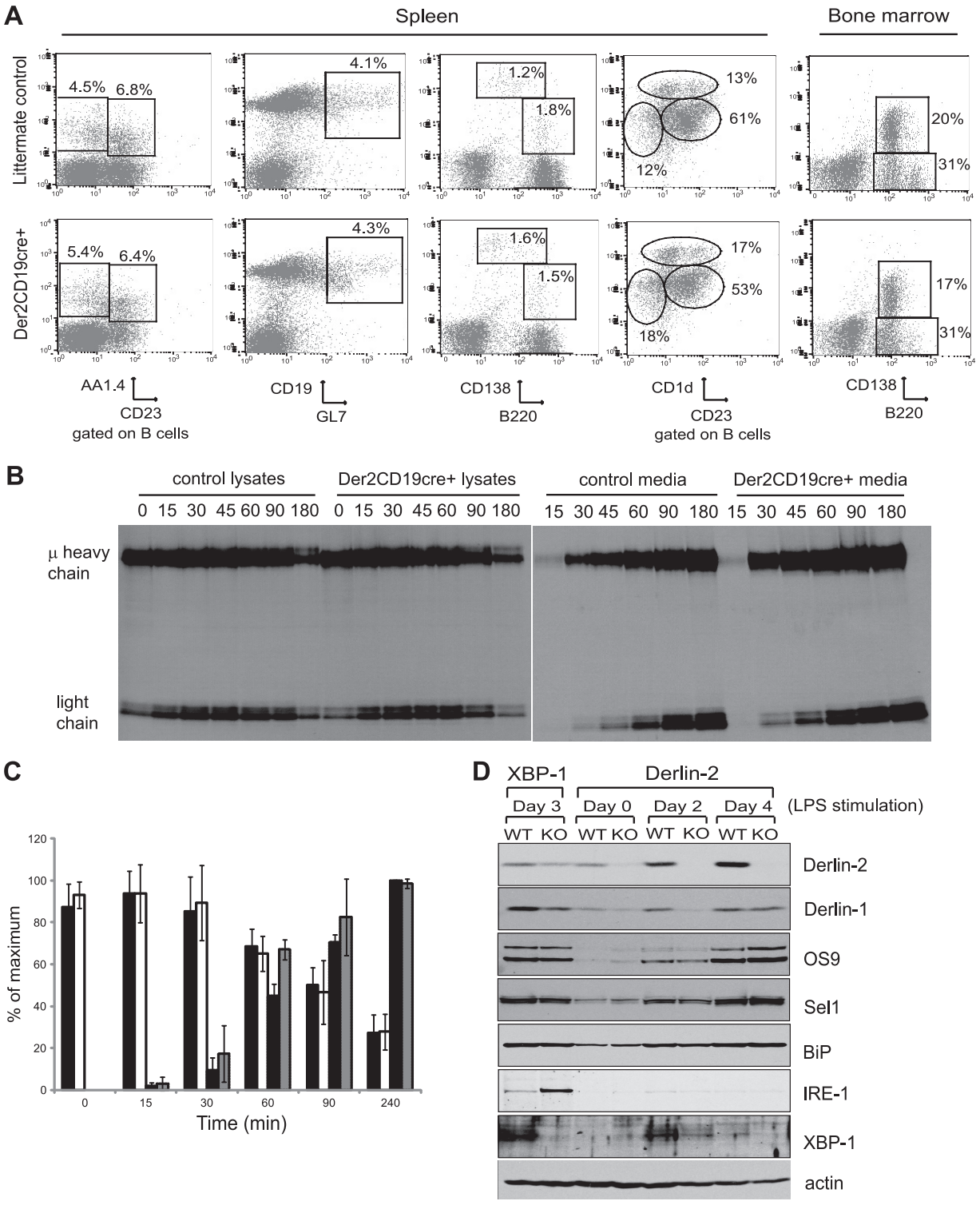

FIG. 4. Derlin-2 deficiency has no effect on B cells. (A) Spleen and bone marrow cells were harvested from *Der2*^{CD19} mice or their Cre-negative littermates. B cell subsets were analyzed by flow cytometry after staining with the indicated antibodies. One representative mouse is shown for each genotype; means for multiple mice can be found in Table 1. (B) B cells were isolated from *Der2*^{CD19} mice or their Cre-negative littermates and cultured for 3 days in medium containing LPS. Cells were then cultured in cysteine- and methionine-free medium for 1 h, pulsed with [^{35}S]cysteine-methionine for 10 min, and chased in nonradioactive medium for the indicated times. Cells were lysed in NP-40 lysis buffer, immunoprecipitated using anti-IgM antiserum, and analyzed by SDS-PAGE. (C) Quantification of three independent experiments performed as described in panel B. Bars (left to right), wt intracellular, *Der2* intracellular, wt secreted, and *Der2* secreted. (D) B cells were harvested from wild-type, *Xbp1*^{CD19}, or *Der2*^{CD19} mice and cultured in medium containing LPS for the indicated number of days. Cells were lysed in NP-40 lysis buffer, subjected to SDS-PAGE, and immunoblotted using the indicated antibodies. KO, knockout.

TABLE 1. Profile of B cell populations in control and *Der2*^{CD19} mice

B cell subset	Marker(s)[a]	% of total cells[b]	
		Control	*Der2*^{CD19}
Marginal zone B cells	CD19$^+$ CD21^{hi} CD23^{lo} CD1d$^+$	9.0 ± 4.2	8.7 ± 4.7
Follicular B cells	CD19$^+$ CD21$^+$ CD23$^+$	61.7 ± 2.7	60.6 ± 3.5
Transitional (T1)	CD23^{lo} AA4.4$^+$	12.0 ± 5.6	10.7 ± 4.4
Transitional (T2)	CD23$^+$ AA4.1$^+$	10.6 ± 6.3	8.4 ± 3.7
Germinal center B cells	CD19$^+$ GL7$^+$	5.6 ± 2.6	4.2 ± 1.5
IgM$^+$ IgD^{lo} spleen cells	IgM$^+$ IgD^{lo}	21.5 ± 4.8	21.2 ± 5.0
IgM$^+$ IgD$^+$ spleen cells	IgM$^+$ IgD$^+$	30.6 ± 10.3	31.8 ± 6.0
IgM^{lo} IgD$^+$ spleen cells	IgM^{lo} IgD$^+$	33.7 ± 11.3	29.3 ± 5.7
CD138$^+$ B220$^+$ spleen cells	CD138$^+$ B220$^+$	3.1 ± 1.2	2.0 ± 1.0
CD138$^+$ B220^{lo} spleen cells	CD138$^+$ B220^{lo}	1.5 ± 0.8	1.1 ± 0.6
Pro-B cells	B220$^+$ CD43$^+$ CD19^{lo}	4.9	5.8 ± 0.4
Pre-B cells	B220$^+$ CD43$^+$ CD19$^+$	24.2	18.4 ± 2.2
Bone marrow plasma cells	CD138$^+$ B220$^+$	19.5 ± 1.1	20.1 ± 4.1
Peritoneal cavity B-1 cells	CD19$^+$ B220^{lo}	11.4 ± 8.5	25.6 ± 10.5

[a] Expression levels of the markers are indicated by superscripts as follows: lo, low expression; hi, high expression.
[b] Percentages of total splenic B cells (first 10 rows), total bone marrow cells (next 3 rows), and total peritoneal cavity cells (last row).

compensatory upregulation in the absence of Derlin-2. OS-9, which was upregulated more than 10-fold in MEFs, was less affected in Derlin-2-deficient hepatocytes. Different tissues must therefore adapt to loss of Derlin-2 in different ways (Fig. 3B and 5G). *Der2*^{Alb} hepatocytes showed increases in IRE-1α and XBP-1s, both of which were somewhat attenuated by starvation. Thus, hepatocytes in *Der2*^{Alb} mice have an ongoing UPR, which is modified only slightly by the nutrient status of the mice (Fig. 5G).

Hepatocytes were isolated from *Der2*^{Alb} mice or their wild-type littermates and cultured *ex vivo* on collagen-coated plates. Metabolic labeling of these primary hepatocyte cultures showed no obvious differences in the profiles of intracellular (Fig. 6A) or secreted proteins (Fig. 6B). Apolipoprotein B is one of the largest proteins synthesized by hepatocytes and is regulated not only by stop transfer sequences that induce ribosome pausing but also by p97-mediated ER dislocation (10, 47). Pulse-chase analysis of apolipoprotein B (apoB-48) showed no differences in the rate of synthesis or secretion of apoB-48 particles or their associated albumin (Fig. 6C and D).

Whole-body deletion of Derlin-2 leads to perinatal lethality and skeletal abnormalities. To achieve complete deletion of Derlin-2, we crossed Derlin-2$^{flox/flox}$ mice to mice transgenic for Cre driven by the CMV promoter. After one generation, the resulting mice were heterozygous for one deleted Derlin-2 allele and one wild-type Derlin-2 allele. Since Derlin-2 is deleted in the germ cells of the heterozygous parents, this breeding strategy ensures that any *Der2*$^{-/-}$ progeny are complete knockouts and do not retain any residual undeleted Derlin-2. Although intercrossing heterozygotes should have yielded *Der2*$^{-/-}$ mice at 25% frequency, *Der2*$^{-/-}$ mice represented only 4% of mice at weaning ($n = 160$). Genotyping of embryos at embryonic day 17.5 to 18.5 showed normal Mendelian inheritance, and no obvious abnormalities were observed in the *Der2*$^{-/-}$ embryos. Closer inspection of *Der2*$^{-/-}$-containing litters revealed several dead or dying pups 24 h after birth, and genotyping of 1-day-old mice with inclusion of the dead or dying pups showed *Der2*$^{-/-}$ mice to be 23.7% of the total. Thus, *Der2*$^{-/-}$ pups are born at Mendelian ratios, but the majority die within 24 h of birth.

To determine the cause of death, several litters containing *Der2*$^{-/-}$ pups were delivered by caesarean section. All pups breathed normally and were not cyanotic, suggesting that lung abnormalities and neural innervation of the diaphragm were not causes of death. Histological analysis of 1-day-old *Der2*$^{-/-}$ pups showed no obvious cause of death, and serial sections of the heart showed no abnormalities (data not shown). The gross structures of the central and peripheral nervous systems and the formation of neuromuscular synapse formation were examined in *Der2*$^{-/-}$ pups and found to be normal (Fig. 7). All neonatal mice are hypoglycemic; *Der2*$^{-/-}$ mice that had been delivered via caesarean section and deprived of food showed no evidence of increased hypoglycemia at 2 h postbirth (Fig. 8A). *Der2*$^{-/-}$ mice that were delivered vaginally and left with their mothers refused to feed. *Der2*$^{-/-}$ pups consistently lacked milk spots and later died of starvation (Fig. 8B). Hand-feeding of *Der2*$^{-/-}$ pups showed that milk could reach the stomach, ruling out structural abnormalities in the upper digestive tract (data not shown). Fostering *Der2*$^{-/-}$ pups to other lactating dams or removal of their wild-type littermates to decrease competition for food did not increase the survival rate of *Der2*$^{-/-}$ pups (data not shown). We conclude that *Der2*$^{-/-}$ pups die perinatally from a failure to feed, with the rare exceptions described below.

Der2$^{-/-}$ mice show massive perinatal death, yet 4% of *Der2*$^{-/-}$ mice from heterozygous crosses do survive to adulthood. Male *Der2*$^{-/-}$ mice were sterile, despite having normal sperm production as assessed by periodic acid-Schiff (PAS) staining of testes (data not shown). Female *Der2*$^{-/-}$ mice were capable of becoming pregnant, but three of three pregnancies ended in late-stage abortions requiring euthanasia of the mother. Thus, all *Der2*$^{-/-}$ mice studied here were generated by intercrosses of heterozygotes. The few surviving *Der2*$^{-/-}$ mice appeared healthy although they were consistently smaller than their littermates as measured by body weight (Fig. 8C) and skeletal length (*Der2*$^{-/-}$, 8.9 ± 0.40 cm; littermates, 9.9 ± 0.42 cm; $P < 0.00001$). Between 2 and 4 months of age, the surviving *Der2*$^{-/-}$ mice developed a striking involution of the rib cage readily detectable by palpation. This involution became progressively worse with age, causing hunching and breathing

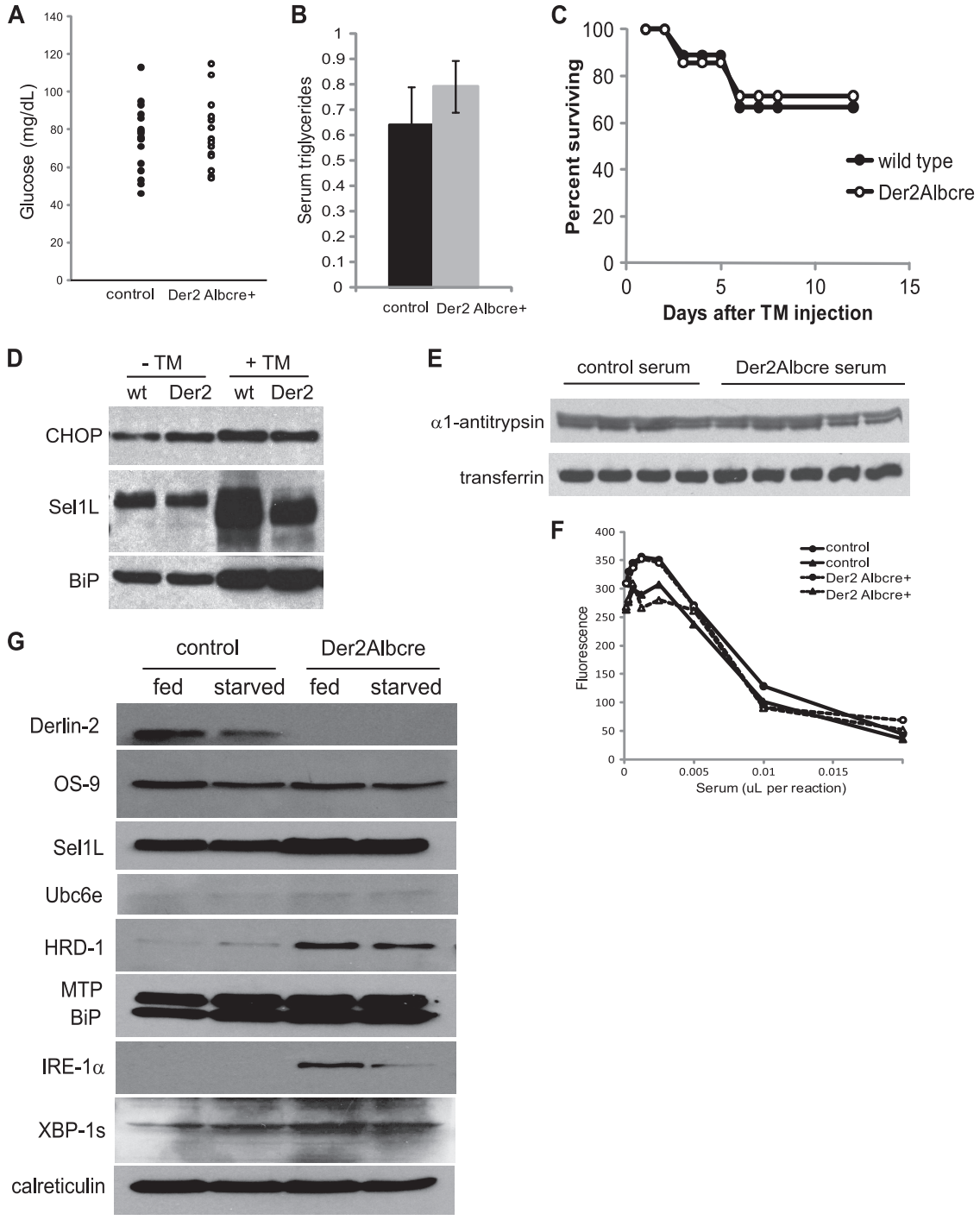

FIG. 5. Derlin-2 deficiency has no effect on liver function. (A) Adult *Der2*^{Alb} mice or their Cre-negative littermates were fasted overnight, and blood glucose levels were measured using a glucose monitoring system. (B) Adult *Der2*^{Alb} mice or their Cre-negative littermates were fasted overnight, and serum triglycerides were measured. (C) *Der2*^{Alb} mice or their Cre-negative littermates were injected intraperitoneally with tunicamycin (1 mg/kg), and body weight was monitored over time. Mice were euthanized when they reached 80% of initial body weight. (D) Mice were injected with TM as described in panel C. Livers were harvested 3 days later, lysed in NP-40 lysis buffer, and immunoblotted using the indicated antibodies. (E) Serum from *Der2*^{Alb} mice or their Cre-negative littermates was subjected to SDS-PAGE and immunoblotted using the indicated antibodies. (F) Serum from two *Der2*^{Alb} mice (dashed lines) and two littermate controls (solid lines) was added to an elastase activity assay to determine the relative levels of inhibitory serum anti-serine proteases. (G) *Der2*^{Alb} mice or their Cre-negative littermates were fasted or not fasted for 24 h. Livers were perfused with PBS, harvested, and lysed in NP-40 lysis buffer. Lysates were subjected to SDS-PAGE and immunoblotted using the indicated antibodies.

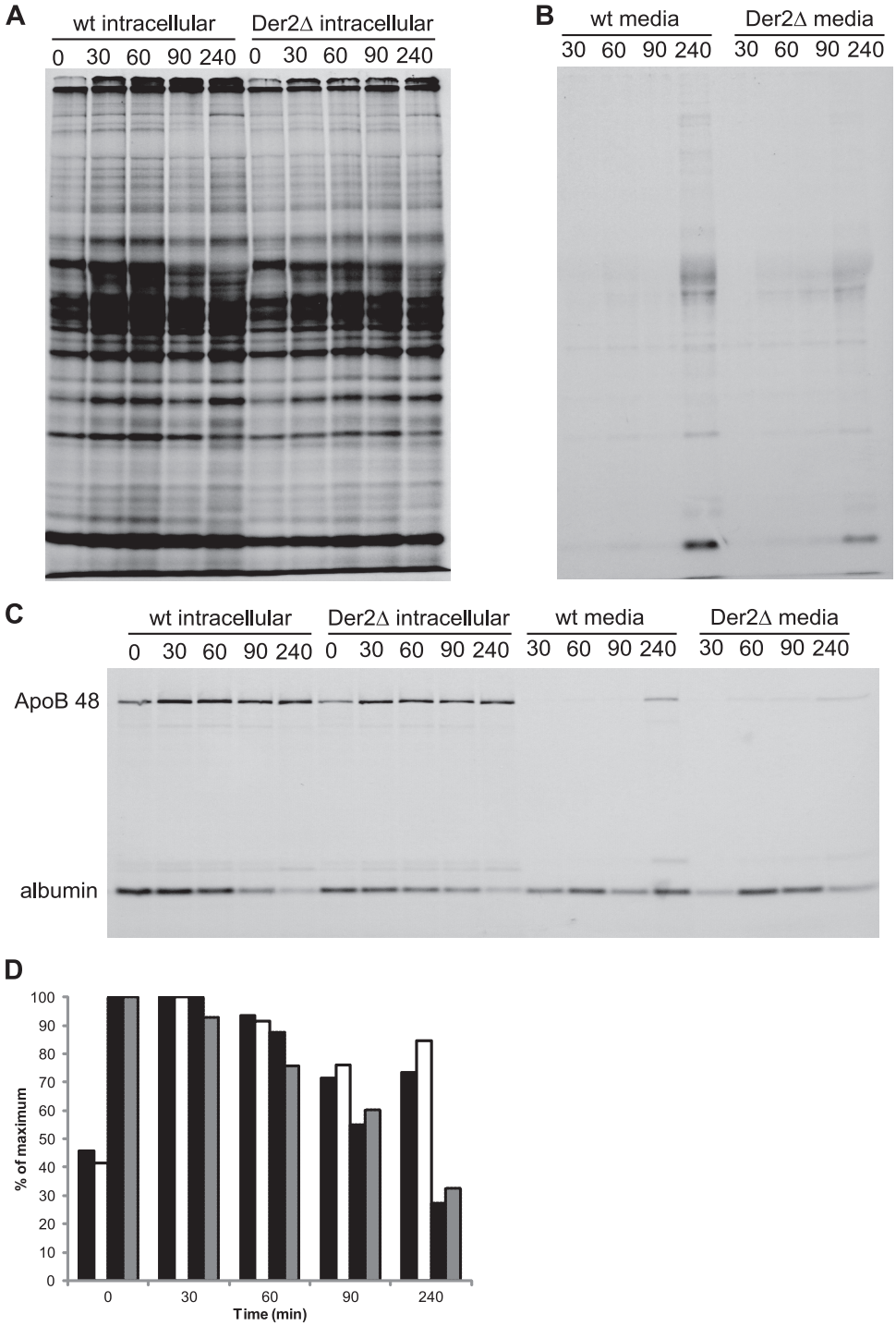

FIG. 6. Derlin-2 deficiency has no effect on protein synthesis in isolated hepatocytes. (A) Hepatocytes were isolated from *Der2*^{Alb} mice (Der2Δ) or their Cre-negative littermates (wild type [wt]). Cells were cultured in cysteine- and methionine-free medium for 1 h, pulsed with [^{35}S]cysteine-methionine for 20 min, and chased in nonradioactive medium for the indicated times. Cells were lysed in NP-40 lysis buffer, and whole-cell lysates were subjected to SDS-PAGE. (B) Hepatocytes were treated as described in panel A, and medium fractions were collected at each time point to assess secreted proteins. Equal volumes of media were subjected to SDS-PAGE. (C) Hepatocytes treated as described in panel A were lysed in NP-40 lysis buffer. Lysates were immunoprecipitated using anti-apolipoprotein B antiserum, and samples were subjected to SDS-PAGE. (D) Quantification of the results of the experiment shown in panel C. Bars (left to right), control ApoB48, *Der2* Albcre plus ApoB48, control albumin, and *Der2* Albcre plus albumin.

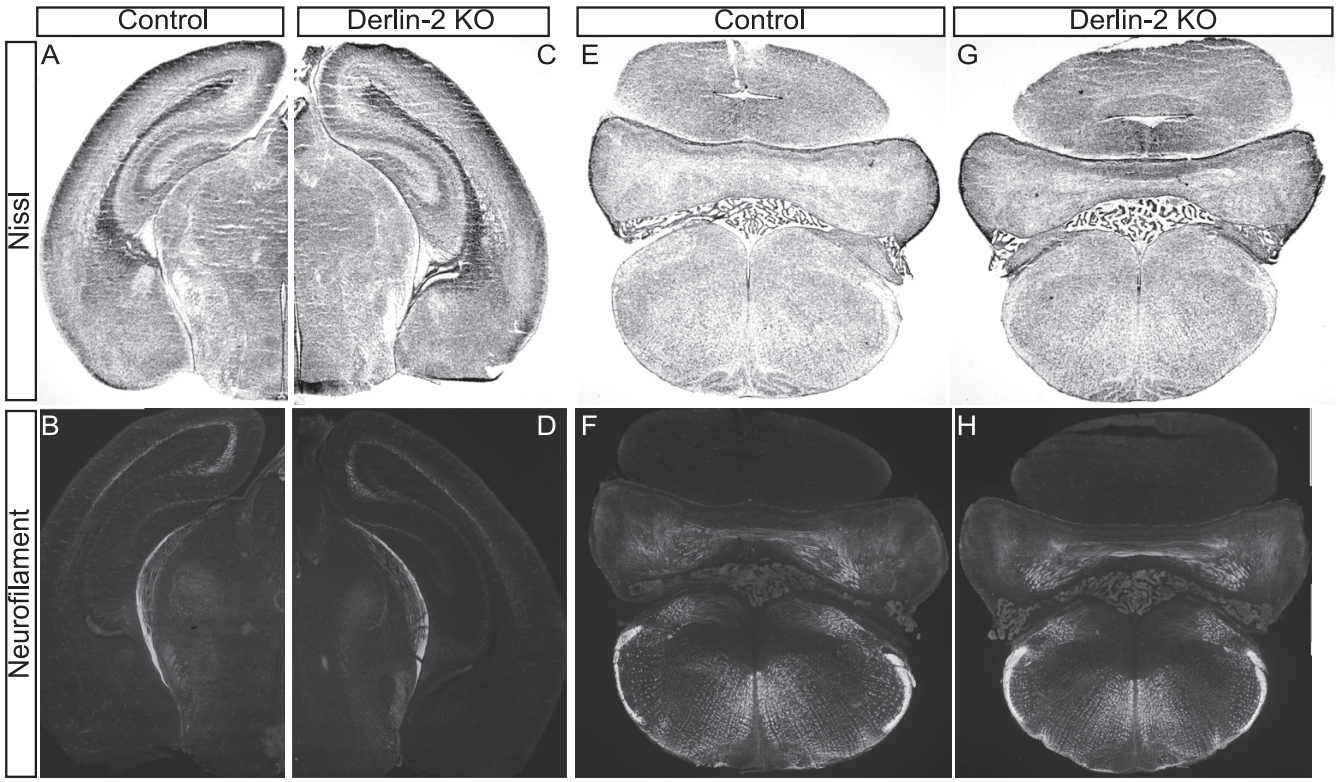

FIG. 7. Nissl and neurofilament staining demonstrate that major axon tracts and the gross structure of the brain are intact at postnatal day 0 in the *Der2*$^{-/-}$ mice (C, D, G, and H) compared to a littermate control (A, B, E, and F). Serial sections from the level of the optic tract (A to D) or from spinal trigeminal nucleus interpolaris (E to H) were stained as indicated. Immunostaining for activated caspase-3 revealed no evidence of increased apoptosis in the central nervous system of *Der2*$^{-/-}$ animals (data not shown). Peripheral nerves and spinal ganglia were also not grossly affected by the loss of Derlin-2. Phrenic innervation of the diaphragm was normal as was the appearance of neuromuscular junctions as determined by whole-mount immunohistochemistry of diaphragm muscle (data not shown). KO, knockout; WT, wild type.

difficulties due to reduced lung volume. Aged *Der2*$^{-/-}$ mice also developed a wasting disease, likely due to their poor overall health status and reduced ability to obtain food. By 12 months of age, all *Der2*$^{-/-}$ mice had to be euthanized.

Skeletons from adult *Der2*$^{-/-}$ mice stained with Alizarin red and Alcian blue showed normal bone and joint formation, with the singular exception of the costal cartilage. *Der2*$^{-/-}$ mice display fusion of the third and fourth sternebrae and develop linear calcifications perpendicular to the axis of rib and periodic nodular thickenings (Fig. 8D). To determine when cartilage abnormalities first appeared, skeletal preparations were made from embryonic day 18.5 fetuses. By day 18.5 of gestation, wild-type mice showed clear divisions of all sternebrae; however, the third and fourth sternebrae showed slightly delayed separation in *Der2*$^{-/-}$ mice (Fig. 8E). No rib abnormalities could be detected in fetal or in 1-day-old *Der2*$^{-/-}$ mice. Thus, defects in cartilage formation are mild at birth and grow progressively worse over time. Given the progressive nature of cartilage defects and the lack of internal hemorrhage in *Der2*$^{-/-}$ pups, we conclude that cartilage defects are unlikely to account for the acute perinatal lethality observed in *Der2*$^{-/-}$ mice. Histological evaluation of adult *Der2*$^{-/-}$ ribs showed a defect in cartilage structure with abnormal chondrocytes (Fig. 8F). In addition, many *Der2*$^{-/-}$ chondrocytes contained eosinophilic cytoplasmic inclusions, suggesting a defect in protein secretion or degradation (Fig. 8G).

Derlin-2-deficient chondrocytes show intracellular retention of extracellular matrix components. The skeletal defects in *Der2*$^{-/-}$ mice phenocopy those of mice transgenic for mutant collagen oligomeric matrix protein (COMP) (35). COMP mutations in humans lead to either pseudoachondroplasia or multiple epiphyseal dysplasia, diseases marked by short stature and weakened cartilage (5, 15). Secreted COMP normally forms pentamers and, along with collagen IX and matrilin-3, binds to collagen II fibrils. In chondrocytes that express mutant COMP, the intracellularly retained COMP nucleates collagen II fibrils in the ER, causing ER dilation, upregulation of CHOP, and ultimately death of the chondrocyte (35). Analysis of *Der2*$^{-/-}$ chondrocytes by electron microscopy likewise revealed ER dilations consistent with intracellular retention of collagen matrix proteins (Fig. 9A and B). These ER dilations were observed in *Der2*$^{-/-}$ chondrocytes that had been grown in three-dimensional culture for 1 day or 8 days (Fig. 9B). After 18 days of culture, virtually all *Der2*$^{-/-}$ chondrocytes were dead, while wild-type chondrocytes were still viable (data not shown). To determine whether ER stress was related to the increase in chondrocyte death, we analyzed expression of CHOP, an apoptosis-inducing protein that is a downstream target of the unfolded protein response. CHOP upregulation was observed in chondrocytes that had been cultured for 8 days (Fig. 9C). CHOP transcripts were also upregulated in primary chondro-

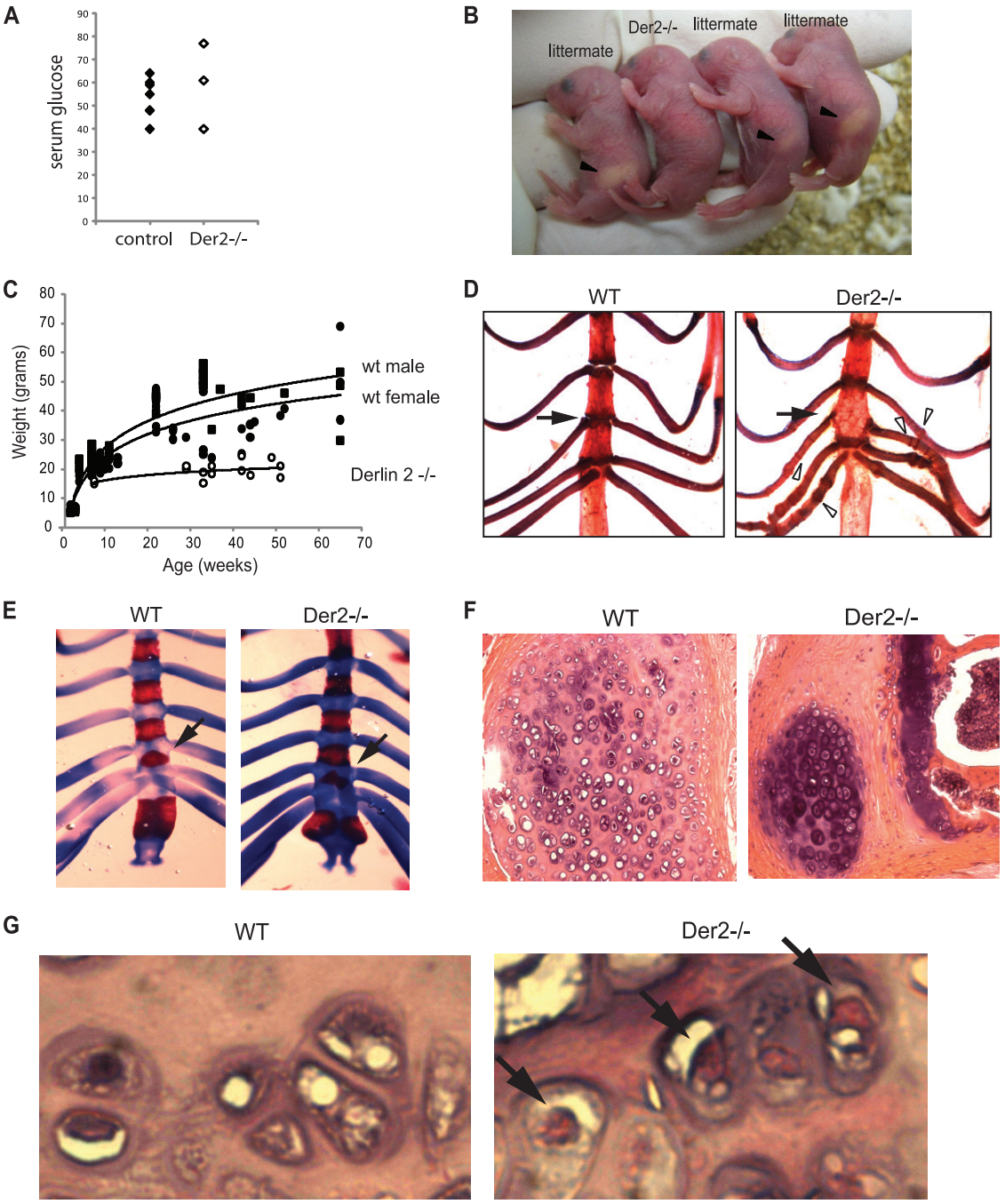

FIG. 8. Whole-body deletion of Derlin-2 leads to perinatal lethality and cartilage defects. (A) One-day-old pups from a litter containing a *Der2*$^{-/-}$ mouse. Note the milk spots (arrowheads) in control mice and the absence of a milk spot in the *Der2*$^{-/-}$ mouse. (B) A litter containing *Der2*$^{-/-}$ pups was delivered via caesarean section and not permitted to feed for 2 h. Serum glucose levels were measured. (C) Body weights of *Der2*$^{-/-}$ mice and their littermate controls at various ages. *Der2*$^{-/-}$ mice did not survive beyond 52 weeks. *Der2*$^{-/-}$ male and female mice did not vary significantly in their weights. (D) Skeletal lengths (nose to base of tail) of adult *Der2*$^{-/-}$ and age-matched littermate control mice were measured. (E) Skeletons of a 9-month-old *Der2*$^{-/-}$ and wild-type control mice were harvested and stained with Alizarin red and Alcian blue. Note the bottom three pairs of ribs connect to a single sternebra in the *Der2*$^{-/-}$ mouse, indicating fusion of the third and fourth sternebrae (arrow). *Der2*$^{-/-}$ rib cartilage is punctuated with linear calcifications (open arrowheads). (F) Skeletons were harvested from embryonic day 18.5 *Der2*$^{-/-}$ and wild-type embryos and stained with Alizarin red and Alcian blue. Note that the ossification center (arrow) between the third and fourth sternebrae is smaller in *Der2*$^{-/-}$ mice. (G) Hematoxylin and eosin staining of rib cartilage from adult wild-type and *Der2*$^{-/-}$ mice (×20 magnification). (H) Sections were prepared as described for panel G. Arrows indicate chondrocytes with eosinophilic cytoplasmic inclusions in adult *Der2*$^{-/-}$ mice. WT, wild type.

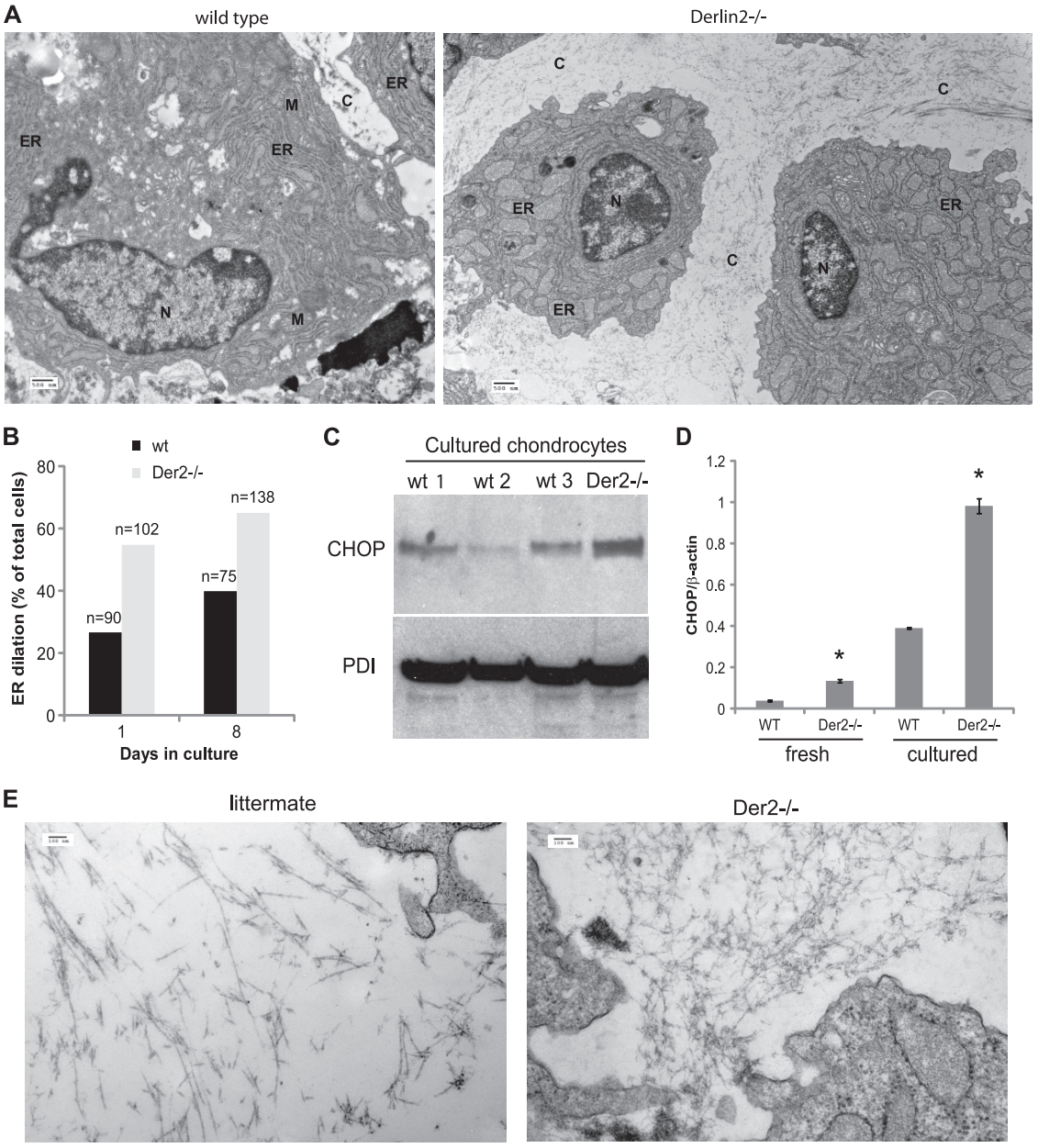

FIG. 9. *Der2*$^{-/-}$ chondrocytes show intracellular retention of extracellular matrix proteins. (A) Chondrocytes isolated from wild-type or *Der2*$^{-/-}$ embryonic day 18.5 mice were maintained in 3D pellet culture for 8 days prior to fixation, sectioning, and analysis by EM. The samples contained similar amounts of extracellular collagen fibrils. Note the distended ER in *Der2*$^{-/-}$ chondrocytes. N, nucleus; M, mitochondrion; C, collagen fibers. (B) Chondrocytes were cultured as described for panel A for 1 day or 8 days. Cells were analyzed by electron microscopy and scored as dilated or not dilated. Total number of cells (*n*) counted per group is indicated above each bar. Results are representative of two independent sample sets. (C) Protein lysates were harvested from chondrocytes that had been cultured for 8 days. Lysates were analyzed by SDS-PAGE and immunoblotted using the indicated antibodies. Note the increased CHOP expression in *Der2*$^{-/-}$ chondrocytes. (D) RNA was isolated from freshly isolated embryonic day 18.5 chondrocytes or chondrocytes that had been maintained in culture for 2 weeks, and cDNA was prepared. Quantitative PCR was performed using primers specific for *Chop* and normalized to β-*actin*. *, $P < 0.005$. (E) Chondrocytes from wild-type or *Der2*$^{-/-}$ embryonic day 18.5 mice were maintained in 3D culture for 8 days and analyzed by EM. Shown are collagen fibrils secreted into the extracellular matrix (×49,000 magnification). The samples contained similar amounts of collagen fibrils.

cytes isolated freshly from embryonic day 18.5 *Der2*$^{-/-}$ sternums as well as in cultured chondrocytes (Fig. 9D), suggesting an increase in chondrocyte apoptosis *in vivo* and not simply a cell culture effect. Both *Der2*$^{-/-}$ and wild-type chondrocyte cultures contained collagen fibrils, and no differences in fibril length or diameter were observed by EM (Fig. 9E). Thus, *Der2*$^{-/-}$ chondrocytes are capable of at least some collagen secretion while alive, which is consistent with the mild, progressive nature of the structural abnormalities seen in *Der2*$^{-/-}$ mice. We therefore conclude that skeletal defects observed in

Der2$^{-/-}$ mice are most likely the result of abnormal ER retention of collagen matrix proteins and a consequent increase in chondrocyte apoptosis.

DISCUSSION

The normal pathways of protein quality control may be compromised either by a reduction in protein folding capability or by the failure to remove misfolded proteins from the ER. Genetic ablation of ER chaperones is often lethal (31). Genetic deletion of some of the known components of the dislocation complex would be expected to lead to a blockade in dislocation or to a failure to remove proteins from the ER. The Derlin family of proteins provides an attractive target for such attempts at interference since they have not been linked to any normal cellular functions other than ER dislocation. We chose to generate Derlin-2 conditional knockout mice because Derlin-2 is ubiquitously expressed and is the strongest interacting partner of the ER-resident ubiquitin ligase HRD1/Sel1L.

Der2$^{-/-}$ MEFs show impaired dislocation of the misfolded substrate RI332, in accordance with data obtained using a dominant negative version of Derlin-2 and short hairpin RNA (shRNA) approaches to knock down expression of *Der2*. Derlin-2 was not required for dislocation of NHK, which is supported by findings that alterations in Sel1L or OS-9, two components known to interact with Derlin-2, have little effect on NHK dislocation (2, 7), yet this was inconsistent with a previous report using Derlin-2-silenced human cells (32). This discrepancy could be explained by species-specific differences or by the fact that other members of the dislocation complex are constitutively upregulated in *Der2*$^{-/-}$ MEFs. *Der2*$^{-/-}$ MEFs showed strong induction of UPR components, implying the accumulation of misfolded proteins in these cells, although we have yet to determine the identity of candidate misfolded proteins in these MEFs. However, the extent to which induction of the UPR is caused by accumulation of misfolded proteins or is engaged by other malfunctions in the ER is not easily ascertained. With the exception of B cells, all *Der2*$^{-/-}$ cell types and tissues examined showed tonic induction of the UPR, with tissue-specific differences in the upregulation of the various components. Known members of the dislocation complex showed compensatory upregulation in *Der2*$^{-/-}$ cells. Sel1L, HRD-1, and Ubc6e levels were elevated in almost every cell type examined. OS-9 levels were higher in *Der2*$^{-/-}$ MEFs and chondrocytes but showed little expression in hepatocytes or B cells. Derlin-1, which is known to form hetero-oligomeric complexes with Derlin-2 (23), was downregulated in *Der2*$^{-/-}$ cells. Derlin-1/Derlin-2 (Derlin-1/2) complexes may form the transmembrane pore through which misfolded substrates traverse the ER bilayer (22, 44). In the absence of Derlin-2, Derlin-1 channels may be less stable, leading to decreased Derlin-1 protein levels in these cells. In the absence of Derlin-2, misfolded proteins become trapped in the ER and so induce the unfolded protein response.

The physiological consequences of a constitutively active UPR have not been addressed previously. In most tissues, a tonic UPR has no obvious adverse consequences. Cells of the B lymphocyte lineage, including plasma cells which apparently are among the most highly active secretory cells in the body, are unaffected by loss of Derlin-2. Hepatocytes, another highly active secretory cell type, are similarly unaffected by the absence of Derlin-2. *Der2*$^{-/-}$ MEFs survive in tissue culture without overt signs of distress. One possible explanation is that functional redundancy in the Derlin family allows for Derlin-1 or Derlin-3 to substitute for loss of Derlin-2. This particular question cannot be decisively answered without a Derlin-1/2/3 triple knockout mouse. Strikingly, Derlin-1 levels are decreased in all Derlin-2-deficient tissues examined, which would argue against the ability of Derlin-1 to substitute for Derlin-2. Derlin-3 is limited in its tissue expression, being primarily located in the placenta and pancreas (32). We detected strikingly little Derlin-3 in hepatocytes, suggesting that the lack of phenotype in these cells is not due to Derlin-3 function. A tonic increase in expression of proteins associated with dislocation is apparently required by *Der2*$^{-/-}$ cells to thrive. How exactly these upregulated proteins contribute to homeostasis remains to be explored in detail. Contrary to expectations, *Der2*$^{-/-}$ mice are born at Mendelian ratios and die perinatally from a failure to feed. How protein quality control could be related to a failure to feed is currently unclear. Nonetheless, Derlin-2 is not required for survival since roughly one-fifth of the expected *Der2*$^{-/-}$ mice from heterozygous crosses reach adulthood. The few surviving *Der2*$^{-/-}$ mice are normal in most respects, despite having a tonic UPR in all tissues. In fact, the only cells obviously affected by absence of Derlin-2 were costal cartilage chondrocytes. These results illustrate the remarkable homeostatic regulation exerted over protein quality control.

What could cause the observed cartilage defect in *Der2*$^{-/-}$ mice? Chondrocytes express Derlin-2 at levels similar to those seen in most other tissues, and although Derlin-1 levels are reduced in *Der2*$^{-/-}$ chondrocytes, Derlin-1 is not altogether absent. Chondrocytes are highly active secretory cells, but why other cells with an equally high secretory burden should be unaffected by loss of Derlin-2 is not immediately obvious. One possible explanation is that collagen matrix proteins are exquisitely sensitive to errors in protein folding. Knockout mice for COMP or matrilin-3 have virtually no phenotype, yet mice transgenic for point mutations in these same proteins develop skeletal dysplasias (18, 20, 35, 38). Small amounts of misfolded collagen matrix proteins can lead to huge deposits of fibrillar collagen in the ER and cause decreased collagen secretion, culminating in death of the affected chondrocytes. *Perk*$^{-/-}$ mice develop skeletal abnormalities due to inadequate secretion of collagen I by osteoblasts, a cell type that expresses unusually high levels of PERK. Dense granules, presumably composed of collagen fibrils, accumulate in the ER of *Perk*$^{-/-}$ osteoblasts (46). Thus, we speculate that *Der2*$^{-/-}$ chondrocytes accumulate extracellular matrix proteins in the ER, leading to distension of the ER and death of the affected chondrocytes. The progressive loss of chondrocytes with age would explain the progressive nature of the cartilage defects in *Der2*$^{-/-}$ mice.

To our knowledge, the *Der2*$^{-/-}$ mouse is the first example of a viable mouse uniquely deficient in a component involved in protein dislocation. Sel1L-deficient mice have been reported which are embryonic lethal around embryonic day 13.5 due to brain and liver abnormalities (11, 21); similarly, loss of HRD-1 results in lethality at embryonic day 13.5 due to failure of hematopoiesis in the fetal liver (41). However, the lack of viable pups and the fact that Sel1L plays regulatory role in Notch signaling complicate the use of these models for study-

ing the role of dislocation in a whole organism. Loss of Derlin-2 impedes dislocation of a subset of misfolded proteins and could be partially compensated by residual Derlin-1. Although whole-body deletion of Derlin-2 results in perinatal lethality, with few animals surviving to adulthood, conditional deletion of Derlin-2 will allow further study of the role of protein dislocation in particular organs or tissues of interest.

ACKNOWLEDGMENTS

S.K.D. is supported by a fellowship from the Cancer Research Institute. H.L.P. is supported by grants from the National Institutes of Health and from the Ellison Foundation.

REFERENCES

1. **Adachi, Y., et al.** 2008. ATF6 is a transcription factor specializing in the regulation of quality control proteins in the endoplasmic reticulum. Cell Struct. Funct. **33:**75–89.
2. **Bernasconi, R., T. Pertel, J. Luban, and M. Molinari.** 2008. A dual task for the Xbp1-responsive OS-9 variants in the mammalian endoplasmic reticulum: inhibiting secretion of misfolded protein conformers and enhancing their disposal. J. Biol. Chem. **283:**16446–16454.
3. **Bertolotti, A., et al.** 2001. Increased sensitivity to dextran sodium sulfate colitis in IRE1β-deficient mice. J. Clin. Invest. **107:**585–593.
4. **Bertolotti, A., Y. Zhang, L. M. Hendershot, H. P. Harding, and D. Ron.** 2000. Dynamic interaction of BiP and ER stress transducers in the unfolded-protein response. Nat. Cell Biol. **2:**326–332.
5. **Briggs, M. D., et al.** 1995. Pseudoachondroplasia and multiple epiphyseal dysplasia due to mutations in the cartilage oligomeric matrix protein gene. Nat. Genet. **10:**330–336.
6. **Calfon, M., et al.** 2002. IRE1 couples endoplasmic reticulum load to secretory capacity by processing the XBP-1 mRNA. Nature **415:**92–96.
7. **Cattaneo, M., et al.** 2009. Functional characterization of two secreted SEL1L isoforms capable of exporting unassembled substrate. J. Biol. Chem. **284:**11405–11415.
8. **Chaudhuri, T. K., and S. Paul.** 2006. Protein-misfolding diseases and chaperone-based therapeutic approaches. FEBS J. **273:**1331–1349.
9. **Ernst, R., B. Mueller, H. L. Ploegh, and C. Schlieker.** 2009. The otubain YOD1 is a deubiquitinating enzyme that associates with p97 to facilitate protein dislocation from the ER. Mol. Cell **36:**28–38.
10. **Fisher, E. A., L. R. Lapierre, R. D. Junkins, and R. S. McLeod.** 2008. The AAA-ATPase p97 facilitates degradation of apolipoprotein B by the ubiquitin-proteasome pathway. J. Lipid Res. **49:**2149–2160.
11. **Francisco, A. B., et al.** 2010. Deficiency of suppressor enhancer Lin12 1 like (SEL1L) in mice leads to systemic endoplasmic reticulum stress and embryonic lethality. J. Biol. Chem. **285:**13694–13703.
12. **Harding, H. P., et al.** 2001. Diabetes mellitus and exocrine pancreatic dysfunction in *perk*$^{-/-}$ mice reveals a role for translational control in secretory cell survival. Mol. Cell **7:**1153–1163.
13. **Harding, H. P., Y. Zhang, and D. Ron.** 1999. Protein translation and folding are coupled by an endoplasmic-reticulum-resident kinase. Nature **397:**271–274.
14. **Haze, K., H. Yoshida, H. Yanagi, T. Yura, and K. Mori.** 1999. Mammalian transcription factor ATF6 is synthesized as a transmembrane protein and activated by proteolysis in response to endoplasmic reticulum stress. Mol. Biol. Cell **10:**3787–3799.
15. **Hecht, J. T., et al.** 1995. Mutations in exon 17B of cartilage oligomeric matrix protein (COMP) cause pseudoachondroplasia. Nat. Genet. **10:**325–329.
16. **Hu, C. C., S. K. Dougan, A. M. McGehee, J. C. Love, and H. L. Ploegh.** 2009. XBP-1 regulates signal transduction, transcription factors and bone marrow colonization in B cells. EMBO J. **28:**1624–1636.
17. **Kaser, A., et al.** 2008. XBP1 links ER stress to intestinal inflammation and confers genetic risk for human inflammatory bowel disease. Cell **134:**743–756.
18. **Ko, Y., et al.** 2004. Matrilin-3 is dispensable for mouse skeletal growth and development. Mol. Cell. Biol. **24:**1691–1699.
19. **Lee, A. H., N. N. Iwakoshi, and L. H. Glimcher.** 2003. XBP-1 regulates a subset of endoplasmic reticulum resident chaperone genes in the unfolded protein response. Mol. Cell. Biol. **23:**7448–7459.
20. **Leighton, M. P., et al.** 2007. Decreased chondrocyte proliferation and dysregulated apoptosis in the cartilage growth plate are key features of a murine model of epiphyseal dysplasia caused by a *matn3* mutation. Hum. Mol. Genet. **16:**1728–1741.
21. **Li, S., A. B. Francisco, R. J. Munroe, J. C. Schimenti, and Q. Long.** 2010. SEL1L deficiency impairs growth and differentiation of pancreatic epithelial cells. BMC Dev. Biol. **10:**19.
22. **Lilley, B. N., and H. L. Ploegh.** 2004. A membrane protein required for dislocation of misfolded proteins from the ER. Nature **429:**834–840.
23. **Lilley, B. N., and H. L. Ploegh.** 2005. Multiprotein complexes that link dislocation, ubiquitination, and extraction of misfolded proteins from the endoplasmic reticulum membrane. Proc. Natl. Acad. Sci. U. S. A. **102:**14296–14301.
24. **Loureiro, J., and H. L. Ploegh.** 2006. Antigen presentation and the ubiquitin-proteasome system in host-pathogen interactions. Adv. Immunol. **92:**225–305.
25. **Lu, P. D., H. P. Harding, and D. Ron.** 2004. Translation reinitiation at alternative open reading frames regulates gene expression in an integrated stress response. J. Cell Biol. **167:**27–33.
26. **Luo, S., C. Mao, B. Lee, and A. S. Lee.** 2006. GRP78/BiP is required for cell proliferation and protecting the inner cell mass from apoptosis during early mouse embryonic development. Mol. Cell. Biol. **26:**5688–5697.
27. **McGehee, A. M., et al.** 2009. XBP-1-deficient plasmablasts show normal protein folding but altered glycosylation and lipid synthesis. J. Immunol. **183:**3690–3699.
28. **Molinari, M., V. Calanca, C. Galli, P. Lucca, and P. Paganetti.** 2003. Role of EDEM in the release of misfolded glycoproteins from the calnexin cycle. Science **299:**1397–1400.
29. **Mueller, B., E. J. Klemm, E. Spooner, J. H. Claessen, and H. L. Ploegh.** 2008. SEL1L nucleates a protein complex required for dislocation of misfolded glycoproteins. Proc. Natl. Acad. Sci. U. S. A. **105:**12325–12330.
30. **Mueller, B., B. N. Lilley, and H. L. Ploegh.** 2006. SEL1L, the homologue of yeast Hrd3p, is involved in protein dislocation from the mammalian ER. J. Cell Biol. **175:**261–270.
31. **Ni, M., and A. S. Lee.** 2007. ER chaperones in mammalian development and human diseases. FEBS Lett. **581:**3641–3651.
32. **Oda, Y., et al.** 2006. Derlin-2 and Derlin-3 are regulated by the mammalian unfolded protein response and are required for ER-associated degradation. J. Cell Biol. **172:**383–393.
33. **Reimold, A. M., et al.** 2000. An essential role in liver development for transcription factor XBP-1. Genes Dev. **14:**152–157.
34. **Reimold, A. M., et al.** 2001. Plasma cell differentiation requires the transcription factor XBP-1. Nature **412:**300–307.
35. **Schmitz, M., et al.** 2008. Transgenic mice expressing D469Delta mutated cartilage oligomeric matrix protein (COMP) show growth plate abnormalities and sternal malformations. Matrix Biol. **27:**67–85.
36. **Shamu, C. E., and P. Walter.** 1996. Oligomerization and phosphorylation of the Ire1p kinase during intracellular signaling from the endoplasmic reticulum to the nucleus. EMBO J. **15:**3028–3039.
37. **Sriburi, R., S. Jackowski, K. Mori, and J. W. Brewer.** 2004. XBP1: a link between the unfolded protein response, lipid biosynthesis, and biogenesis of the endoplasmic reticulum. J. Cell Biol. **167:**35–41.
38. **Svensson, L., et al.** 2002. Cartilage oligomeric matrix protein-deficient mice have normal skeletal development. Mol. Cell. Biol. **22:**4366–4371.
39. **Todd, D. J., A. H. Lee, and L. H. Glimcher.** 2008. The endoplasmic reticulum stress response in immunity and autoimmunity. Nat. Rev. Immunol. **8:**663–674.
40. **Wu, J., et al.** 2007. ATF6α optimizes long-term endoplasmic reticulum function to protect cells from chronic stress. Dev. Cell **13:**351–364.
41. **Yagishita, N., et al.** 2005. Essential role of synoviolin in embryogenesis. J. Biol. Chem. **280:**7909–7916.
42. **Yamamoto, K., et al.** 2007. Transcriptional induction of mammalian ER quality control proteins is mediated by single or combined action of ATF6alpha and XBP1. Dev. Cell **13:**365–376.
43. **Ye, Y., et al.** 2005. Inaugural article: recruitment of the p97 ATPase and ubiquitin ligases to the site of retrotranslocation at the endoplasmic reticulum membrane. Proc. Natl. Acad. Sci. U. S. A. **102:**14132–14138.
44. **Ye, Y., Y. Shibata, C. Yun, D. Ron, and T. A. Rapoport.** 2004. A membrane protein complex mediates retro-translocation from the ER lumen into the cytosol. Nature **429:**841–847.
45. **Zhang, K., et al.** 2005. The unfolded protein response sensor IRE1α is required at 2 distinct steps in B cell lymphopoiesis. J. Clin. Invest. **115:**268–281.
46. **Zhang, P., et al.** 2002. The PERK eukaryotic initiation factor 2α kinase is required for the development of the skeletal system, postnatal growth, and the function and viability of the pancreas. Mol. Cell. Biol. **22:**3864–3874.
47. **Zhou, M., E. A. Fisher, and H. N. Ginsberg.** 1998. Regulated co-translational ubiquitination of apolipoprotein B100. A new paradigm for proteasomal degradation of a secretory protein. J. Biol. Chem. **273:**24649–24653.
48. **Zinszner, H., et al.** 1998. CHOP is implicated in programmed cell death in response to impaired function of the endoplasmic reticulum. Genes Dev. **12:**982–995.